The application of X-ray computed tomography to the characterisation of pyrometallurgical products – a case study

Corfield, A.A., Chetty, D., Mukadi, J. and Bisaka, K.

Mintek, Private Bag X3015, Randburg, 2125, South Africa

Corresponding author: deshc@mintek.co.za

Smelting is an important process for the production of a number of commodities once primary processing and upgrading have been completed. Key factors for consideration include the feed composition, but also furnace conditions. Components, such as electrodes, refractory linings and the physical attributes of the feed, need to be carefully considered for peak performance and safety of the operation. To date, mineralogical/phase-chemical characterisation of such components has been two-dimensional in nature, relying on the preparation of large, resin-impregnated, polished slabs for characterisation using microscopy in a time-consuming and often inaccurate manner. In this paper, we consider the advantages of 3D X-ray computed tomography over traditional microscopy for characterisation of a Soderberg electrode. Particular emphasis is placed on the characterisation of porosity distribution, which has implications for the physical and electrical stability of these electrodes in the smelting environment.

KEYWORDS

X-ray tomography, Soderberg electrode, porosity, density

1. INTRODUCTION

A Soderberg electrode is a continuously-formed electrode used in an electric arc furnace, in which a blended mixture of dry carbon aggregate, such as anthracite, and a tar or pitch binder is fed into a steel casing and melted into a paste, after which it is baked to form a solid conductor. During the heating process, when the carbon undergoes graphitisation and volatile materials are driven off, pore spaces are formed, impacting the density of the material. The heating process used, and the composition and density of the material produced in this way, has a bearing on its performance in service, in terms of mechanical strength and electrical conductivity (Hogue *et al*., 1954).

Porosity measurements were performed on samples cut from different intervals along a baked electrode using optical microscopy. These measurements are time-consuming and considered inaccurate in characterising large-scale porosity distribution effects. Attention therefore turned to three dimensional (3-D) analysis using microfocus X-ray computed tomography (XCT). The theory behind XCT is explained in a number of publications (e.g. Kak and Slaney, 1999; Ketcham and Carlson, 2001), and is not repeated here.

2. MATERIALS AND METHODS

2.1. Sampling and preparation for optical microscopy

Samples were taken at specific intervals along the length of a Soderberg electrode section, as shown in Figure 1.

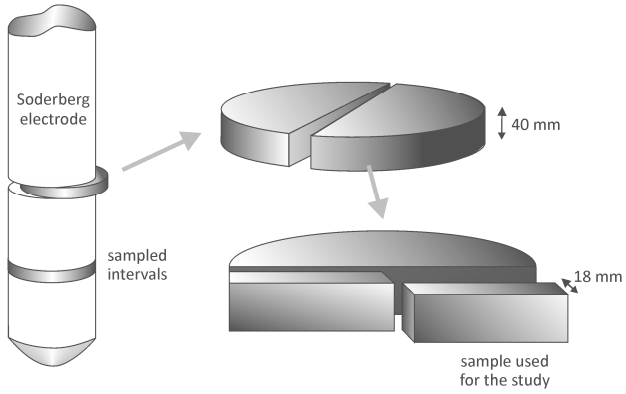

Figure 1. Sampling of Soderberg electrode

These samples were sectioned to expose a cross sectional slice of the electrode extending from the outer edge of the electrode to its centre, a length of 100 mm. Four sections with an area of approximately 18 x 18 mm^2 each were cut along the length of each slice (Figure 2) and vacuum embedded in epoxy resin prior to polishing for examination using an optical microscope.

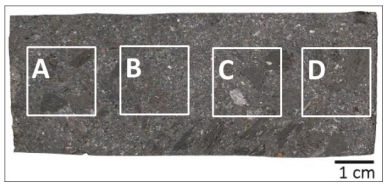

Figure 2. Image of one half of the electrode sample showing the location of samples taken for the polished sections used for point counting by optical microscopy.

Conventional optical point counting methods were used to measure the porosity. This involved the counting of pores relative to the electrode material on each of the

polished sections, by moving the sample stage in precise stepped intervals on an optical microscope and recording the material (sample or pore space, now filled with epoxy resin) observed under the cross hair. This was repeated until 1500 points had been measured.

2.2. Tomography study

A Soderberg electrode section was sampled in the same way as before, as shown in Figure 1. Instead of slicing the sample into 4 individual sections for polishing, however, a slab, in the form of a rectangular prism measuring approximately 18 x 18 x 100 mm^3 was cut from the electrode half. Figure 3 shows a typical electrode portion used for the XCT study.

Figure 3. Appearance of a typical sample slab used for the XCT study. The sample length is 100 mm.

The samples were imaged using with a Nikon HMX ST Computed Tomography system with a 225 KV micro-focus X-ray source and a 14 bit real time detector. The excitation conditions employed were 70 kV and 125 µA, given the low density of the material. Each sample slab was imaged in two passes (first the outer 50 mm portion

and then the inner 50 mm portion). A total of 4000 image projections was performed on each pass with a resultant voxel size of 31.8 µm.

The grey scale images obtained clearly distinguish the porosity from the material of the electrode (graphite, oxide or silicate phases and metal/alloy particles).

The tomogram or image stack was processed using ImageJ, a public domain, Java-based image processing program. It was possible, utilising this software, to apply greyscale thresholding to the image stack to produce binary images that represent the pores within the sample. The binary image stacks were then processed to obtain the extent of porosity in the samples.

Using ImageJ it was evident that free space on the outside of the sample would be included in calculations of porosity owing to an undefined outer boundary of the sample. For this reason, an inner volume, or region of interest, was extracted from the sample and this was used for all porosity calculations. Another advantage of this approach is that all slices in the tomogram would have exactly the same dimensions in terms of surface area and volume, facilitating uniform data handling.

In contrast to the optical point counting method, which only measured four surface areas across the radius of each electrode, up to 3000 transverse slices of the sample slab were measured along the length of each sample by this method.

2.3. Bulk density determination

The bulk density was determined in two ways: by the classical method using weight and volume measurement and, utilising the 3-D image volume, by applying an average solids density value to the non-porous material in each image slice.

For the classical method the sample slab was precision cut into smaller rectangular prisms with approximate dimensions of 18 x 18 x 24 mm^3 and dried in a laboratory oven. After cooling, the dimensions and mass of each rectangular prism were measured and recorded. Afterwards the density of each of the four rectangular prisms was calculated by dividing the mass of each by their volume.

For the 3-D study the image stack was measured in four evenly spaced sequential clusters to match the volumes measured by the classical method. Since the true density of the solid material in the Soderberg electrode was unknown, the density of the solids in the sample slabs first had to be determined. A volume of sample of the same size as the rectangular prism used for the tomography study was cut from the opposite radius of the Soderberg electrode and used for this purpose. The volume and mass was determined by measuring the cooled, oven dried slab. The entire sample was then pulverised. A representative sub-sample was loaded into a Micromeritics AccuPyc II 1340 Gas Pycnometer to establish the true density of the electrode material. This density value was then applied to the solid portion of each slice in the image stack and the total bulk density calculated for each quarter along the length of the sample slab (to correspond with the classically determined bulk density measurements).

3. RESULTS AND DISCUSSION

3.1 Porosity distribution

The conventional method of point counting on an optical microscope requires samples to be cut from a cross section of the electrode that are then mounted in epoxy resin, ground and polished to produce a two dimensional plane for observation and measurement. The quality of the information obtained is dependent on the number of sections measured. Such an approach is time-consuming, however, and therefore expensive, both to prepare a large number of polished sections and to carry out optical point counting on them. Furthermore it is a destructive process since the samples are encapsulated in epoxy resin and cannot be recovered for any subsequent work that may be necessary.

Specific details of the optical point counting study are not discussed here, except to highlight the limitation of time for observation and counting, as well as the need for substantial sample preparation to achieve more representative and statistically valid results. In contrast, tomography offers the possibility that many more areas can be measured rapidly and more cost effectively.

Figure 4 shows the typical appearance of an image slice from the tomogram. It illustrates the appearance of the original sample area from the raw tomogram and the corresponding region of interest that was selected for subsequent calculations of area and volume.

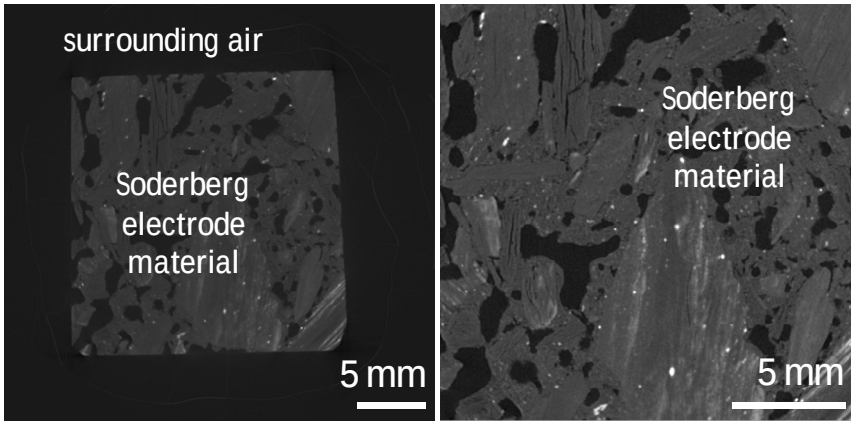

Figure 4. Original tomogram image slice (left) and region of interest area (right) used for subsequent analysis. The dominant dark grey is graphite and the pores are black. Light grey phases are other phases whereas the white specks are alloy, typically iron.

The rectangular prism electrode sample was scanned in two passes to image the two halves corresponding with the inner and outer portions of the electrode, in order to obtain a desirable image resolution. Two volumes, therefore, were generated for each sample. Each consisted of ~1500 slices, giving ~3000 slices for the total sample volume. The image sequencing is stylistically depicted in Figure 5.

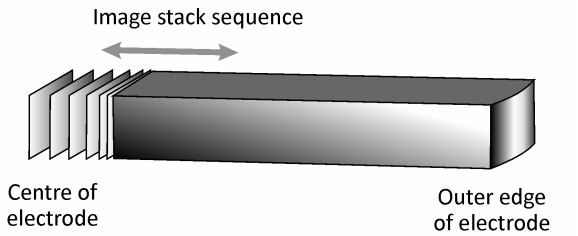

Figure 5. Stylistic portrayal of a typical sequence of slices taken from the tomogram or image stack. There is 0.032 mm distance between each image.

In the tomogram image slices, the pore space in the samples has the lowest grey levels, i.e., nearest to black, since the pores contain air, which has the lowest linear

coefficient of attenuation. The sample itself exhibits a range of grey level brightness commensurate with phase composition based on the linear attenuation coefficient.

The darkest portions of the image were isolated from the rest of the sample by greyscale thresholding. The lower end of the threshold is set at zero while the upper end is advanced until all the apparent pore space is consumed. The largest pores have distinct grain boundaries and are therefore easily assigned within the threshold range. The process becomes somewhat subjective when fine structural detail is present in some of the graphite particles. In ImageJ it is possible to move through the tomogram to observe and evaluate the effectiveness of the threshold level on all of the images in the stack. Once the level is settled, the setting may be applied and the proportion of pore space calculated for the entire stack. It is this fine detail, bordering on the resolution of the images, which is the limiting factor of the current method.

Three samples were studied in detail. The analysis of one particular sample is given here as an example and is typical of all the samples examined.

The measurements of the area assigned to pores in each image of the image stack are shown graphically in Figure 6(A). Note the variation of porosity within the sample from the centre to the outside edge of the electrode. This is owed to the presence of variably-sized aggregate particles in the Soderberg paste and how their presence affects and directs the flow of gases through the electrode during the heating process.

Images representing varying amounts of porosity in the sample in specific regions, indicated by arrows in Figure 6(A), are shown in Figure 7.

Optical point counting on four polished sections, each with a surface area of 18 x 18 mm^2, encompasses a total surface area of 5.4 cm^2. By contrast, a 3-D-study can cover many times that area. Using the same quantity of sample, the example presented here covered an equivalent area of 7 487 cm^2 (16.5 x 16.5 mm^2 x 2716 image slices).

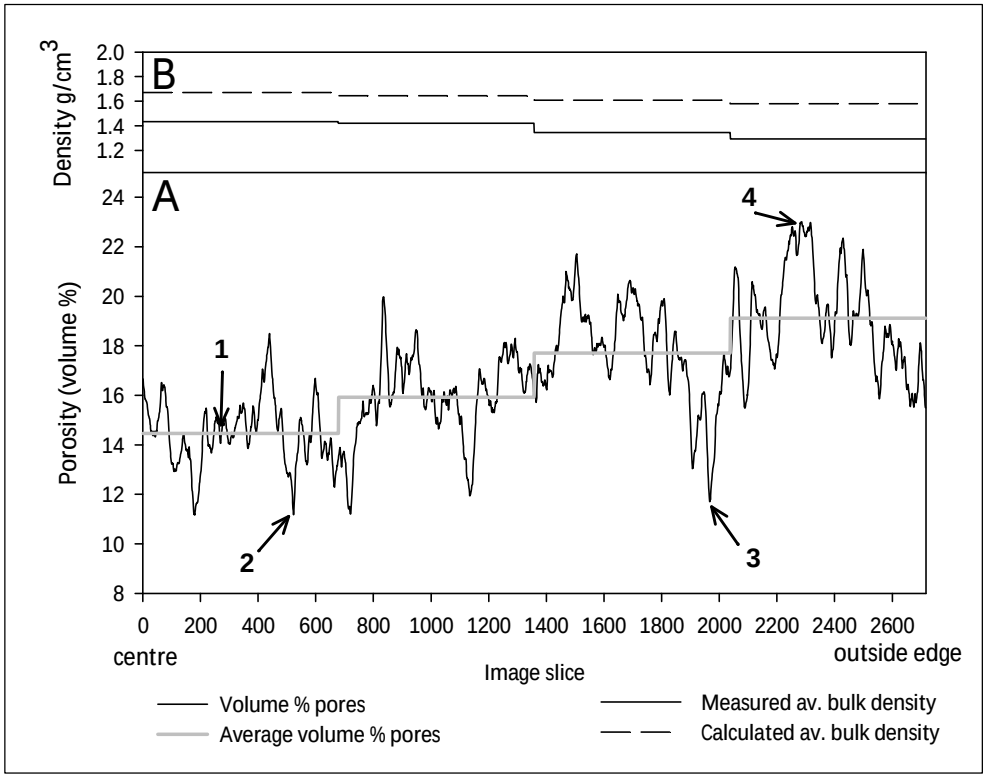

Figure 6. (A) Porosity measured from image slices of a typical cross section of a Soderberg electrode. (B) Measured average bulk density vs. Calculated average bulk density. The numbers refer to images shown in Figure 6.

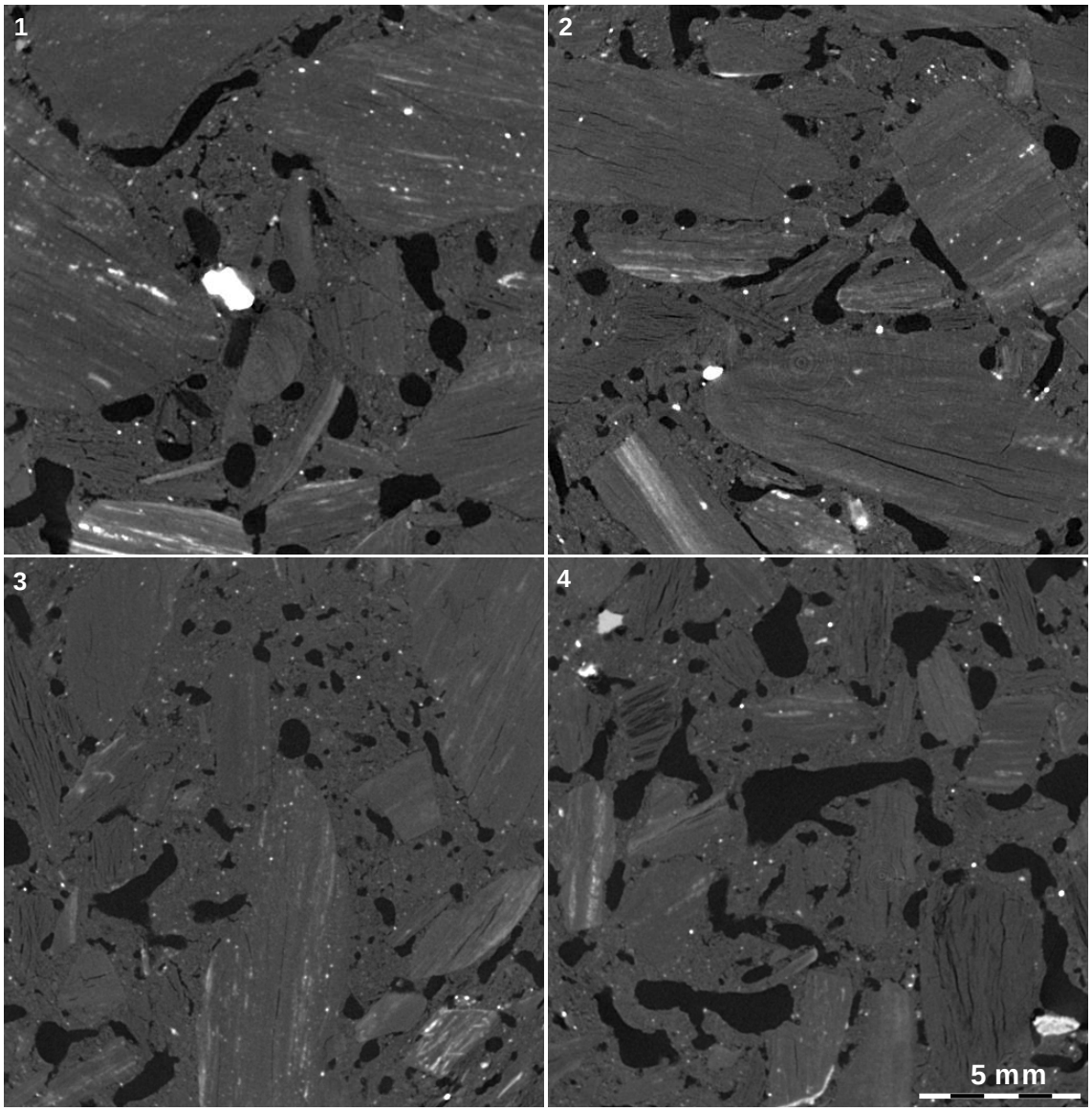

Figure 6. Images of specific slices taken from the Soderberg electrode (indicated by arrows in Figure 6), illustrating the variation in porosity (black) The main phase is graphite whereas the brighter phases are either metallic Fe (white) or metal oxides or metal silicates (various shades of light grey).

3.2 Bulk density

The results of the density measurements on the four rectangular prisms are presented in Table 1. Table 2 shows the bulk density measurement of the rectangular prism that was subsequently pulverised for the true density

determination. The density measurement of this sample is in agreement with the average bulk density of the smaller rectangular prisms. The result of the true density determination (Table 3) was used for the calculation of bulk densities from the XCT porosity data (Table 4).

Table 1. Bulk density determination of four small rectangular prisms of a Soderberg electrode, measured by conventional means

Sample	Mass (g)	Volume (cm^3)	Bulk density (g/cm^3)
A (centre)	10.16	7.09	1.43
B	10.28	7.23	1.42
C	10.39	7.73	1.35
D (outside)	9.44	7.31	1.29
Total	40.28	29.36	1.37

Table 2. Bulk density, measured by conventional means, of a rectangular prism sample of a Soderberg electrode used for the true density measurement.

Mass (g)	Volume (cm^3)	Bulk density (g/cm^3)
47.71	34.76	1.37

Table 3. True density of a representative milled portion of the rectangular prism sample of Table 2, determined using a gas pycnometer

Mass of sample (g)	Temperature (°C)	True density (g/cm^3)
5.01	19.2	1.95

The bulk density of the solids in the image slices was calculated by applying the true density to the average solids portion of the images (100 % - volume% of porosity).

The measured average bulk density results shown in Table 1 were used for comparison, with relative errors presented in Table 4. The density values are plotted in Figure 6(B), to show the expected inverse relationship with porosity distribution.

Table 4. Measured bulk density and calculated relative density of sequential clusters of images, their differences and relative error

Sample	*Average sample Solids Volume %	Measured average bulk density (g/cm^3)	Calculated average bulk density (g/cm^3)	**Δ** density (g/cm^3)	Relative error %
A (centre)	85.54	1.43	1.67	0.24	16.8
B	84.08	1.42	1.64	0.22	15.5
C	82.30	1.35	1.60	0.25	18.5
D (outside)	80.89	1.29	1.58	0.29	22.5

* 100 % - volume % of porosity

The bulk density data obtained by applying a true density value to the solids component of the Soderberg electrode images produces a relative error of up to 22.5 % in this specific example.

The measured porosity values are likely lower than actual porosity present in the sample. The reason for this is that fine porosity (<30 µm) is present in the samples and it is not possible to resolve these delicate structures using image greyscale thresholding. For the same reason, the calculated bulk density is also higher than in reality because the unmeasured fine pores would contribute towards the solids proportion, increasing the calculated bulk density. Higher resolution imaging is possible but a balance should be struck between the need for it and cost. Despite this limitation, XCT provides advantages of cost saving with less sample preparation and analytical time, and statistical accuracy over conventional optical point-counting.

Using the image stack it would be further possible to evaluate the nature of the porosity, including pore shapes and sizes, spatial distribution of pores, etc. Using the contrast between different phases in the images, it is possible to evaluate the quantity, size and distribution of metallic particles within the electrode, as well as to characterise the variety of oxide and other phases present. It is also possible to graphically present the data in a variety of three-dimensional ways to allow greater clarity in visualising specific problems and envisioning their solutions.

4. CONCLUSIONS

It is important that the composition and structure of Soderberg electrodes conform to desired specifications, which are dependant to a large extent on the porosity and density of the material. These measurements are thus key parameters in understanding the mechanical, electrical conductivity and thermophysical properties of Soderberg electrodes.

Optical point counting is a useful technique for measuring porosity in samples. It is, however, time consuming to perform in terms of sample preparation and in performing an adequate number of measurements. Soderberg electrodes have variable particle size distribution necessitating a large number of measurements to achieve reasonable accuracy. Interception of all features present in the samples is unlikely without extensive sample preparation.

X-Ray computed tomography offers an alternative to the optical point counting approach. It is rapid, and non-destructive, permitting subsequent further analysis of

the same sample to be performed, since sample integrity is maintained. Over the same period of time (a few hours), an XCT study is able to examine significantly larger volumes than a limited point counting study would represent, without the added stereological complications associated with 2-D study.

The results presented, show good agreement between 3-D data and classical density measurement methods, making it suitable for ascertaining porosity distribution at a larger scale than would be feasible for 2-D methods.

The XCT technique may be applied to examine a range of other pyrometallurgical materials such as refractory bricks and linings, as well as the briquetting or pelletizing of products, to examine, for example, particle packing density, the effects of calcination, sintering and firing, etc.

5. ACKNOWLEDGEMENTS

Mr Paul Keanly of X-Sight X-Ray Services CC is acknowledged for acquiring the X-ray measurements of samples and reconstructing the tomograms.

6. REFERENCES

Hogue, R.S., Westlake, R.L. and Moga, G.M. (1954) Carbon and graphite electrodes evaluated for use in Ferroalloy furnaces, Journal of metals, 6, 1379.

Image J: http://rsb.info.nih.gov/ij/ Accessed August 2012.

Kak, A.C., and Slaney, M., Principles of computerised tomographic imaging. The institute of Electrical and Electronics Engineers, Inc., New York, 1999. 329 pp.

Ketcham, R.A., Carlson, W.D., Acquisition, optimization and interpretation of X-ray computed tomographic imagery: Applications to the geosciences. Computers and Geosciences 27 (4), 2001, 381-400.